Scheduling Impact on the Performance of Relay-Enhanced LTE-A Networks

Mattia Minelli, Maode Ma, Marceau Coupechoux, and Philippe Godlewski

***Abstract*—This paper studies the performance of two traditional schedulers, Proportional Fair (PF) and Round Robin (RR), in the context of relay-enhanced LTE-A networks. These two schedulers are indeed natural candidates for implementation in relays nodes (RN) and, following the results obtained in single-hop networks, mobile operators could be tempted to adopt PF because of the good trade-off it offers between cell capacity and fairness. Based on a statistical throughput evaluation model, we show that this is not necessarily the right option. The number of RNs, their locations in the cell, and the backhaul link quality have indeed a decisive influence on the scheduler choice. In some scenarios, it is even not desirable to deploy relays as they degrade the network performance compared to the no relay case. For the purpose of performance evaluation, we develop a realistic and computationally tractable statistical network model that takes into account fast fading, multiple interferers, cell range expansion bias, backhaul link quality, and traffic load. We also propose an optimization of the radio frame structure and a sub-optimal RN placement scheme in order to fairly compare RR and PF.**

I. Introduction

Multi-hop relay networks are regarded as a solution to increase coverage and capacity of cellular networks [1], [2], following the growing demand for mobile Internet and wireless multimedia applications, and the ITU-R/IMT advanced requirements for 4G systems [3]. Relay Nodes (RN) are part of the Release R10 of LTE-A (Long Term Evolution Advanced). The deployment of RNs gives the network a hierarchical structure, where User Equipments (UE) can access the network directly through the eNode-B (eNB) or via a RN [4].

In this paper, we propose a performance evaluation methodology for relay-enhanced LTE-A networks making use of an optimized relay placement heuristic. We particularly focus on the impact of scheduling by comparing Proportional Fairness (PF) and Round Robin (RR) policies. Desirability of relaying with respect to single-hop networks is assessed as in some scenarios deploying RNs degrades the network performance. Moreover, our study analyzes the effect of the eNB-RNs link (i.e., the *backhaul link*) on performance, which is deemed a major performance bottleneck of relay-based networks [5]. To this purpose, two types of backhaul link are considered: the *out-of-band* backhaul and the *in-band* backhaul.

M. Minelli and M. Ma are with the Nanyang Technological University, Nanyang Avenue, Singapore (e-mail: mattia1@e.ntu.edu.sg, emdma@ntu.edu.sg). M. Minelli is also with Télécom ParisTech and CNRS LTCI, 46, rue Barrault, Paris, France.

M. Coupechoux and P. Godlewski are with Télécom ParisTech and CNRS LTCI, 46, rue Barrault, Paris, France (e-mail:{marceau.coupechoux, philippe.godlewski}@telecom-paristech.fr.).

A. Related Work

Performance of Orthogonal Frequency Division Multiple Access (OFDMA) relay-based networks has been treated in a number of works. Uplink and downlink relay-enhanced networks performance is the topic of, e.g., [6]. In this study, RNs are located close to the cell edge, and cell coverage extension is evaluated by means of simulations. Authors consider the opportunity of *biasing* the serving station assignment towards RNs, so as to expand relay cell range (also known as *Cell Range Expansion* (CRE) [7]) and thus increase the number of UEs served by RNs. Results show a consistent performance improvement obtained by load balancing the traffic between eNBs and RNs. However, authors consider only out-of-band relaying, and RNs locations are arbitrarily chosen.

Reference [8] copes with the planning and optimization of relay-enhanced cellular networks. It proposes a simplified analytical model for cell capacity evaluation, based on approximating UEs Signal to Interference plus Noise Ratios (SINR) with the ratio of serving station received power and dominant interferer received power. Using this approximation, authors derive expressions for, e.g., ideal RNs-eNB distance, mean cell capacity, cell edge capacity and optimal RN number. Another study based on a dominant interferer SINR model is given in [9], which analyzes the impact of different in-band backhaul link design approaches on users rate and cell coverage. Analytical formulas for the Probability Distribution Function (PDF) and Cumulative Distribution Function (CDF) of UEs and backhaul rates are derived. Using these expressions, the paper shows that RNs deployment brings a consistent performance improvement. Authors assume that each RN serves one UE, and no UEs are directly served by the eNB. Hence, effect of scheduling and cell load on performance is not captured. Moreover, the single-interferer model (also adopted in [8]) may yield inaccurate results, especially in an urban scenario, where several interferers may impair useful signal reception. Here also [8], [9], RN positions are arbitrarily chosen. This is a common assumption in papers related to relay-based cellular networks, e.g., [9], [10], [11], [12], [13], [14] and [15], where RNs are uniformly located on a circle centered at the eNB. While this assumption may be reasonable when, e.g., few RNs are deployed, it may lead to an inconvenient RN arrangement when the number of RNs grows.

The comprehensive work [13] deals with the self-optimization of RN networks, and contains a section on RNs performance. The role of backhaul link is highlighted, by considering a variable propagation constant on the backhaul links, and a fixed propagation constant on the UEs-related links. Results show that relaying is desirable only if the difference between the propagation constant on UEs-related links and that on the backhaul links is higher than a threshold. However, optimization does not consider RNs positioning and CRE. Moreover, performance evaluation is here focused on average cell spectral efficiency, as well as in [8] and [16]. Hence, it does not account for the effects of cell load and scheduling. This drawback affects [9] as well.

In papers that analyze scheduling impact on performance, the PF scheduler is one of the most adopted, because it reaches a good compromise between overall throughput maximization and fairness in users data rates [17]. Reference [18] introduces a PF scheduling algorithm for multi-hop OFDMA systems and analyzes its performance. Authors derive the NP-hard PF metric maximization problem. Then, they propose a sub-optimal solution based on separating user assignment to nodes and resources scheduling, so as to reduce the algorithm complexity. This paper however does not analyze the scheduling gain and its dependency on network parameters (such as cell dimension and number of RNs) and load. Instead, this topic is dealt with in [19], which focuses on the impact of PF scheduling on multihop cooperative relay networks, and reports derivations of exact and asymptotic performance measures for amplify-and-forward RNs. These measures are obtained from the symbol error rate and outage probability, which are in turn derived from the analytic expression of the SINR CDF. Results show consistent gains, increasing with the number of served UEs. However, no insight is provided on the gain allowed by the PF scheduling, compared to a RR scheduling approach.

A study on outage probability for non-cooperative multihop networks under PF scheduling is performed in [20]. Exact formulas and upper bounds for outage probability are obtained using the SINR CDF on the source-relay link and relay-users links. A similar approach is adopted in [21]. Results show outage for varying number of interferers at the relay and destination, and for varying number of users. In this work, as well as in [19] and [21], RNs serve the UEs with the best instantaneous SINR or best instantaneous received signal. This strategy aims at maximizing the overall throughput, but it suffers from lack of fairness in UE resources scheduling: UEs with a low average SINR or low useful received signal power, e.g., those far away from their serving station, may be assigned a consistently smaller share of radio resources, compared to users experiencing better average radio conditions.

From the results observed in single-hop networks, an operator could be tempted to implement PF for the good trade-off it offers between cell capacity and fairness. However, from the proposed literature, it is not clear whether it should systematically implement PF in its equipments when relays are deployed, or, on the contrary, whether it could rely on the much simpler RR scheduler. In this paper, we investigate in which cases and under which assumptions it happens.

In order to evaluate the performance of these schedulers, we rely in particular on a sub-optimal relay placement scheme. The problem of optimally placing RNs in a cellular network has been tackled in [22]. Paper [22] does not however consider PF scheduling at all and focuses on the structure of the optimal placement using Simulated Annealing, which is a computationally intensive meta-heuristic. The engineering insights obtained by [22] are used here to design a faster placement policy.

B. Contributions

Our main contributions are summarized hereafter:

We compare PF and RR schedulers in relay-enhanced LTE-A networks by relying on a non oversimplified network model (as it is done in several papers). We indeed take into account the effect of fast fading, multiple interferers, cell range expansion bias, backhaul link quality, relay transmit power, traffic load and we propose design bounds for the multi-hop network frame structure (Corollary 1). In order to obtain quick results in various scenarios, fast fading is not explicitly simulated but its statistical effect is taken into account in performance evaluation. We derive formulas for the station average sum physical data rate under RR and PF (Propositions 1 and 2) and give a necessary and sufficient condition of the desirability of RN deployment (Proposition 3). A more realistic interference model is also considered, which brings new insights on RN networks performance and desirability.

Differently from most of the existing literature, we propose a novel RN placement algorithm in order to take into account the impact of RN positioning on performance. Finding the best RN placement is necessary to have a fair comparison between schedulers. However, using traditional meta-heuristic optimization techniques is computationally intensive. On the contrary, our heuristic depends on a single variable, making the optimization process quick and allowing the analysis of a great variety of scenarios.

The role of backhaul quality on RN cellular networks performance is studied, by analyzing different backhaul links scenarios. In the out-of-band case, deploying relays is similar to a network densification and therefore leads to a capacity increase. In the in-band case, we show the crucial impact of the backhaul link capacity not only on the network performance but also on the desirability to deploy relay nodes.

In the case of RN networks, we show that using PF at relays is more demanding in terms of backhaul resources for in-band relaying. Thus, there are conditions, where the scheduling gain is really small or even negative. This type of study for RN cellular networks is novel, to the best of authors knowledge.

The article is organized as follows. Section II describes the adopted system model. Section III proposes a heuristic for the RN placement problem. Section IV analyzes network performance assuming RR and PF scheduling, and derives the optimal frame structure for in-band relays. Section V presents our simulation results and discusses them, while conclusions are finally given in Section VI.

II. System Model

This section includes a description of the network and propagation models, the downlink frame structure and the SINR computation.

A. Network Model

We analyze the downlink of a hexagonal tri-sectorized LTE-A cellular network. Network infrastructure is composed by a set of network *stations*, each labeled with an index k. Two types of stations are considered: eNB sectors and RNs. Every eNB sector controls N_{RN} RNs. We focus on the eNB sector with index $k=0$ and we denote $\mathcal{S}_{RN} \triangleq \{1, ..., N_{RN}\}$ the set of indices of the corresponding RNs. We define $\mathcal{S} \triangleq \mathcal{S}_{RN} \cup \{0\}$. Let $\mathcal{E}$ and $\mathcal{R}$ be respectively the set of all eNB sectors and the set of all RNs in the network. There are N_U UEs in the network, of which N_k are served by station k. Let $\mathcal{U}$ be the set of all UEs and $\mathcal{U}_k$ the set of UEs served by k, so that $\mathcal{U} = \cup_{k \in \mathcal{S}} \mathcal{U}_k$. Network model is represented in Figure 1.

We consider half-duplex decode-and-forward RNs, equipped with omni-directional antennas. RNs forward the data received by the eNB sector antenna to UEs they serve. The link between the eNB sector and RN k is called the Backhaul Link (BL) k. The set of links between RN k and its served UEs is named Relay Link (RL) k. UEs directly served by the eNB sector communicate over the Direct Link (DL).

Each UE is served by the network node providing the highest received (pilot) power; fast fading effect is not considered in the serving station selection process, because the received power is assumed to be averaged on a large number of frames. We define the surface $\mathcal{A}_k$, of area $A_k \triangleq |\mathcal{A}_k|$, as the network region where k is the best server. A coefficient $\mathcal{B}$ (called *bias factor*) can be added to the value of the power received by UEs from RNs, before selecting the serving station: the higher the bias factor, the higher the percentage of UEs served by RNs. This procedure is referred to as *Cell Range Expansion* [7], and it is an effective means to improve cell capacity and coverage (see, e.g., [23], [24], [25], [26], [27]).

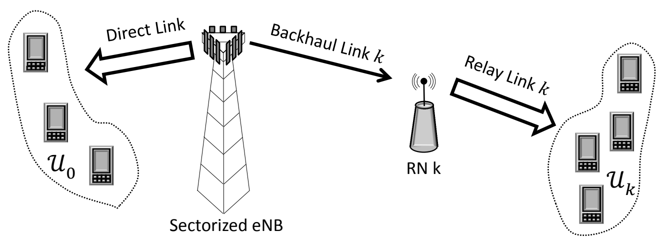

Fig. 1. Network model: RNs are served by a sector of an eNB sector via the Backhaul Link (BL); UEs are served either by the eNB sector via the Direct Link (DL) or by a RN via the Relay Link (RL).

B. Frame Structure

Available downlink radio resources are organized in frames of duration T_F. A frame is a block of contiguous radio resources limited in frequency and time, and divided into several *resource blocks*. Each station transmits its own downlink frame over the same radio resources, and uses a portion of frame resource blocks to serve its RNs and/or UEs.

We consider both in-band and out-of-band relays. When in-band relays are considered, the BL uses the spectrum resources of the operator and is subject to network planning. In this case, let t_a be the quota of frame resource blocks dedicated to RL and DL, and τ the quota of frame resource blocks devoted to transmission on the BL, so that $t_a + \tau = 1$. Resources belonging to quota τ are used by the eNBs on the BL to serve their controlled RNs, and they are orthogonal to resources belonging to quota t_a [28], [29], [30]. Orthogonality is necessary because of the half-duplex nature of RNs. Resources of quota t_a are used by both eNBs and RNs to serve their UEs. Each station can transmit to only one UE or RN per resource block.

We adopt a *static resource partitioning* policy, i.e., t_a and τ are the same in each frame. This approach is not optimal in terms of network performance (see [9]), but processing requirements for the eNB can be considerably reduced, making this solution attractive for operators, and in-cell and inter-cell interference is less variable and unpredictable [30]. Moreover, transmission overheads for resource partitioning-related communications are minimized. Parameter τ can be decomposed into contributions τ_k, each related to the links between eNB sector and RN k: $\tau = \sum_{k=1}^{N_{RN}} \tau_k$. We denote $\underline{\tau} \triangleq (\tau_1, ..., \tau_{N_{RN}})$. The resulting frame structure is represented in Figure 2, for a hypothetical scenario in which one eNB sector serves two RNs ($\mathcal{S}_{RN} = \{1, 2\}$).

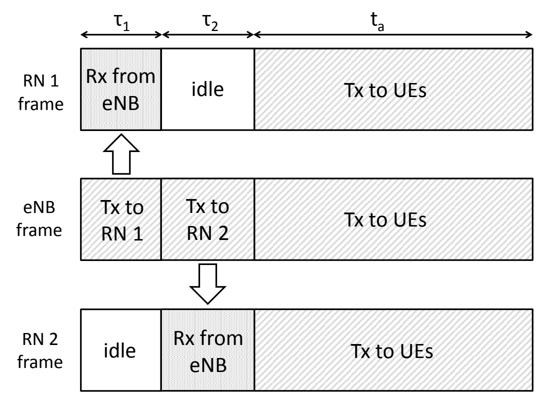

Fig. 2. Frame structure: DL/RL use orthogonal resource blocks with respect to BL, resource partitioning is assumed to be static.

When out-of-band relays are considered, the BL is using another frequency band (e.g. over a microwave link) or a dedicated narrow beam, so that BL radio resources are not subject to the cellular network planning. In this case, $\tau = 0$. These definitions of in-band and out-of-band relays are in accordance with the definitions of the 3GPP [4].

C. Relay and Direct Link Models

A *full buffer* traffic model is adopted, i.e., stations downlink transmission buffers always contain data to be sent to UEs [4]. UEs are randomly located in the network and their position is assumed to be fixed during a frame transmission. We assume a uniform spatial distribution of the UEs[1].

We suppose that all eNB sectors on the one hand, all RNs on the other hand, transmit at the same power per resource block: $P_{tx,0} = P_{eNB}$ and $P_{tx,k} = P_{RN}$, $\forall k \in \mathcal{S}_{RN}$, where $P_{tx,k}$ indicates the transmission power of station k. We denote

[1]This assumption is made for the sake of simplicity but it is not a strict requirement for our model. In case of non uniform distribution, results of Sections IV-B and IV-C should be modified accordingly.

with $P_{rx,i,k}(b,n)$ the power received by UE i from station $k \in \mathcal{S}$ on resource block b of frame n, and we express it as:

$$P_{rx,i,k}(b,n) = P_{tx,k} g_{i,k}(n) \theta_{i,k}^2(b,n), \quad (1)$$

where $g_{i,k}(n)$ is the path gain including distance dependent gain and shadowing and $\theta_{i,k}^2(b,n)$ represents the fast fading effect. The gain $g_{i,k}(n)$ can be written: $g_{i,k}(n) = \frac{K_{i,k}}{r_{i,k}(n)^{\eta_{i,k}}} A_{i,k}(n)\Omega_{i,k}(n)$, where $K_{i,k} \in \{K_{RL}, K_{DL}\}$ is a propagation constant, $\eta_{i,k} \in \{\eta_{RL}, \eta_{DL}\}$ is the path-loss exponent, $r_{i,k}(n)$ is the distance between i and k, $A_{i,k}(n)$ is the antenna gain in the direction of i, and $\Omega_{i,k} = 10^{\frac{\xi_{i,k}}{10}}$ is a lognormal Random Variable (RV) with $\xi_{i,k}$ a normal zero-mean RV of standard deviation $\sigma_{i,k}$. We assume: $\forall (i,k) \in \mathcal{U} \times \mathcal{E}$, $\sigma_{i,k} = \sigma_{DL}$, and $\forall (i,k) \in \mathcal{U} \times \mathcal{R}$, $\sigma_{i,k} = \sigma_{RL}$. We assume that $g_{i,k}(n)$ is constant over a frame duration and across resource blocks.

The fast fading coefficient $\theta_{i,k}(b,n)$ is supposed to follow a Rayleigh distribution, so that $\theta_{i,k}^2(b,n)$ is an exponentially distributed RV with mean 1. We adopt here a Block Rayleigh fading model, i.e., $\theta_{i,k}(b,n)$ is constant on b, while any two realizations on different resource blocks are independent[2]. The average received power $\bar{P}_{rx,i,k}(n)$ on the i-k link, over the resource blocks of frame n can be written as:

$$\bar{P}_{rx,i,k}(n) = \mathbb{E}_{\theta_{i,k}}\left[P_{tx,k} g_{i,k}(n) \theta_{i,k}^2(b,n)\right] = P_{tx,k} g_{i,k}(n), \quad (2)$$

where $\mathbb{E}_{\theta_{i,k}}$ designates the expectation with respect with the random variable $\theta_{i,k}$.

Let now express the Signal to Interference plus Noise Ratio (SINR) experienced by i on resource block b and frame n:

$$\gamma_{i,k}(b,n) = \frac{\bar{P}_{rx,i,k}\theta_{i,k}^2(b,n)}{\sum_{j \in \mathcal{E} \cup \mathcal{R},\, j \neq k} \bar{P}_{rx,i,j}\theta_{i,j}^2(b,n) + N}, \quad (3)$$

where $N = N_0 B$ is the background noise power, with N_0 the thermal noise spectral density and B the resource block bandwidth. For the sake of further developments, we exploit the approximation proposed by authors of [32], [33], [34] for the sum of interferers powers in (3):

$$\sum_{j \in \mathcal{E} \cup \mathcal{R},\, j \neq k} \bar{P}_{rx,i,j}\theta_{i,j}^2(b,n) \approx \sum_{j \in \mathcal{E} \cup \mathcal{R},\, j \neq k} \bar{P}_{rx,i,j}, \quad (4)$$

which follows from the law of large numbers. Accordingly, the SINR can be written as $\gamma_{i,k}(b,n) = \Gamma_{i,k}(n)\theta_{i,k}^2(b,n)$, where $\Gamma_{i,k}(n)$ is equal to:

$$\Gamma_{i,k}(n) = \frac{\bar{P}_{rx,i,k}}{\sum_{j \in \mathcal{E} \cup \mathcal{R},\, j \neq k} \bar{P}_{rx,i,j} + N}, \quad (5)$$

and can be seen as the average SINR experienced by i on frame n.

Finally, we denote with $\rho_{i,k}(b,n)$ the *instantaneous data rate* associated to UE i served by k on resource block b of frame n. This parameter is approximated as in [35]:

$$\rho_{i,k}(b,n) = \min\{\alpha \log_2(1 + \beta \Gamma_{i,k}(n)\theta_{i,k}^2(b,n)),\, \rho_{\max}\}, \quad (6)$$

where α is the bandwidth efficiency factor, β is the SINR efficiency factor (see [35]), and $\rho_{\max}$ is the maximum achievable spectral efficiency. Parameters α, β and ρ_{max} depend on the adopted set of modulation and coding schemes. We denote:

$$R_{i,k}(n) \triangleq \mathbb{E}_{\theta_{i,k}}[\rho_{i,k}(b,n)] \quad (7)$$

the average value of $\rho_{i,k}(b,n)$ over fast fading realizations.

D. Backhaul Link Model

As in [28], we consider only the effect of path-loss and shadowing on signal propagation on the BL. This is justified by the fact that RNs do not move, and network planning is performed on the basis of long-term performance indicators. Hence, the signal power received by RN k from eNB sector h on a given resource block of frame n is equal to

$$\bar{P}_{rx,k,h}(n) = P_{tx,h} g_{k,h}(n), \quad (8)$$

where the shadowing standard deviation on all links between an eNB sector and a RN is equal to σ_{BL}. For performance evaluation of in-band relays, we will consider two backhaul link qualities: a favorable case called 'LOS BL' and an unfavorable case called '3GPP BL' (see Section V-B). The average SINR $\Gamma_{k,h}(n)$ during frame n is given by:

$$\Gamma_{k,h}(n) = \frac{\bar{P}_{rx,k,h}}{\sum_{j \in \mathcal{E},\, j \neq i} \bar{P}_{rx,k,j} + N}, \quad (9)$$

where we used assumption (4) for the interference term. Note that interference on the relay link is uniquely generated by eNBs. Now, the average rate $R_{BL,k}(n)$ achieved by RN k on the BL is approximated as:

$$R_{BL,k}(n) = \min\{\alpha \log_2(1 + \beta \Gamma_{k,h}(n)),\, \rho_{\max}\}. \quad (10)$$

III. Relay Placement Algorithm

When evaluating the performance of a relay-based cellular network, the way relays are placed in the cell plays a crucial role. In this subsection, we thus intend to find a 'good' relay placements in terms of sector throughput for a given pair $(\mathcal{B}, N_{RN})$ of bias and number of relays. The complexity of the objective function seems to exclude standard methods in convex and non-convex optimization theory [36], [37]. The RN location problem includes the capacitated facility location problem as a special case, so that it is NP-hard [38]. Exhaustive search becomes rapidly unfeasible as the number of RNs and RN candidate sites increase. Popular meta-heuristics, such as Simulated Annealing (SA) or Tabu Search, have been adopted in e.g. [39], [22] for relay placement but they also require a high number of computations and anyway provide a sub-optimal solution.

A. Proposed Heuristic

In this paper, based on the experience acquired from our previous work [22], we propose a RN placement heuristic algorithm, which yields sub-optimal but very quick results. The first idea of our proposal is to perform an exhaustive search over a *well chosen* subset of all possible RNs placements. From the results of [22], we can observe that out-of-band relays tends to be located near the cell border, where radio conditions are worst. In-band relays tend to be closer to the

[2]This is a typical assumption in the literature on relays, in physical layer studies, see e.g. [31], as well as in relay planning studies, see e.g. [28].

eNB in order to benefit from a better backhaul link quality. At last, as the number of RNs or their transmit power increase, there is a repulsion effect that tends to create several rings of relays around the eNB.

Relying on these observations, we define a class of relay topologies. Each topology is defined by the pair $(N_{RN}, \bar{d})$, where $\bar{d}$ is the topology reference distance and is defined hereafter. Relays in a given sector are arranged on one or more tiers, which are outlined so as to keep constant the distance between RNs on the same tier, and the distance between a tier and the cell edge (see Figure 3). Parameter $\bar{d}$ represents the distance between two neighboring tiers, the distance between neighboring RNs on the same tier, and the minimum allowed distance between any two RNs in the network. The number of tiers and the number of RNs on each tier is determined by $\bar{d}$, N_{RN} and the cell dimension.

As shown in Algorithm 1, the method proceeds by steps and takes as inputs N_{RN} and $\bar{d}$. At step $g > 0$, a certain number of relays n_r remain to be placed. A new tier at a distance $d_g = (1/2 + (k-1))\bar{d}$ from cell edge is built and $p_g = \min\{n_g; n_r\}$ RNs are placed on it, where n_g is the maximum number of RNs which can be allocated to tier g. This is determined as[3] $n_g = \left\lfloor \frac{l_g}{\bar{d}} + 1 \right\rfloor$, where l_g is the length of tier g. The p_g relays assigned to tier g are arranged so that the distance between one RN and its neighbor is $\bar{d}$, and RN locations are symmetric with respect to the sector antenna boresight direction. The algorithm stops when either all RNs have been placed, i.e., configuration $(N_{RN}, \bar{d})$ is feasible, or $d_g \geq R\sqrt{3}/2$, i.e., configuration $(N_{RN}, \bar{d})$ is not feasible because RNs do not fit into their cell sector, with the given $\bar{d}$.

The idea behind this method is to place RNs on a regular pattern, organized in tiers around eNBs. Small values of $\bar{d}$ lead to RN patterns, in which all RNs are close to each other, and close to the cell border. Large values of $\bar{d}$ produce placements where RNs are more regularly distributed in the sector. Although the proposed algorithm is suboptimal, its advantage lies in the fact that location of all RNs solely depends on one parameter and allows the analysis of a large set of situations.

B. Complexity

We now compare the complexity of the proposed heuristic, the exhaustive search and an example of meta-heuristic usually adopted in the literature, i.e., SA. Optimization is performed over the variations of P_{RN}, $\mathcal{B}$ and the RN locations. The three considered approaches proceed by iterations. At a given iteration of the optimization process, the performance of a configuration is computed. This is by far the more computationally intensive task (compared to the repeat-until loop of Algorithm 1 or the search for a neighbor configuration in SA). This performance evaluation step being common to the three algorithms, the three algorithms are similar in terms of complexity *for a given iteration*. We thus have to compare the number of iterations and the optimality of the obtained results.

Assume that P_{RN} can take P possible values, $\mathcal{B}$ can take B possible values and that there are N_{RN} relays. With the

[3] The function $\lfloor \cdot \rfloor$ yields the highest integer which is lower or equal to the function argument.

Algorithm 1 Relay placement algorithm

```
Input parameters: N_RN, d
Initialization: n_r ← N_RN, g ← 1
repeat
    d_g ← (1/2 + (g − 1)) d,
    if n_r > 0 then
        Outline tier g and compute l_g
        Compute n_g = ⌊l_g/d + 1⌋
        Compute p_g = min{n_g; n_r}
        Place p_g relays on tier g, distanced by d and symmetric wrt antenna boresight direction
        n_r ← n_r − p_g, g ← g + 1
    end if
until n_r == 0 OR d_g ≥ R√3/2
Return: relay placement (n_r == 0) OR 'Configuration not feasible' (d_g ≥ R√3/2)
```

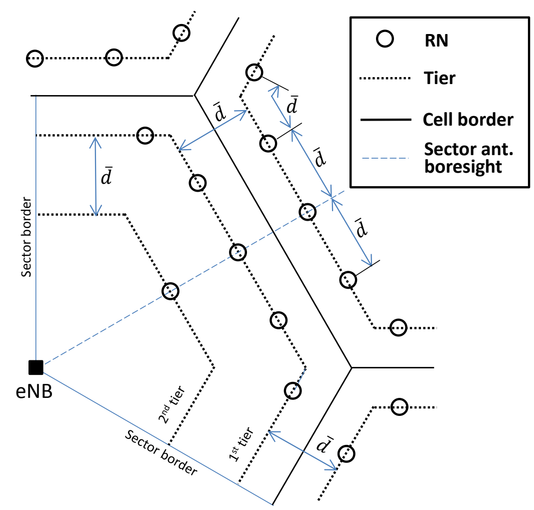

Fig. 3. Proposed RN placement with reference distance $\bar{d}$ and $N_{RN} = 6$.

proposed heuristic, the RN location is obtained by varying $\bar{d}$ in an interval $[x_{min}ISD, x_{max}ISD]$ with a step of $x_{min}ISD$, where ISD is the Inter-Site Distance (the distance between two neighboring eNBs) and $x_{min}, x_{max} \in [0; 0.5]$. This results in D possible values for $\bar{d}$. Whatever the number of relays, we thus obtain $P \times B \times D$ iterations. This is independent on N_{RN}.

Consider now the exhaustive search approach, which consists in testing all possible configurations. If we want the same accuracy in the RN locations, we need to discretize the sector area in elementary surfaces of area $(x_{min}ISD)^2$. The area of a sector is $\frac{ISD^2}{2\sqrt{3}}$. There is thus $\frac{1}{x_{min}^2\sqrt{3}}$ possible locations for a single relay. This results in $\frac{P \times B}{(x_{min}^2\sqrt{3})^{N_{RN}}}$ configurations to test. So this is clear that the proposed heuristic is much less complex than the exhaustive search, although it is sub-optimal.

SA is a meta-heuristic for which it is very difficult to derive accuracy results. There are some works from Olivier Catoni [40], [41], [42] on this question that are based on large deviations theory. This work however cannot be directly applied to our problem because we have a very weak knowledge of the characteristics of the objective function. Note however that the search space of SA is the same as for the exhaustive search and thus includes $\frac{P\times B}{(x_{min}^2\sqrt{3})^{N_{RN}}}$ possible configurations. Both exhaustive search and SA will thus see their efficiency decrease as N_{RN} increases.

IV. Network Performance and Frame Optimization

This section is devoted to the analysis of the network performance in terms of sector sum throughput under PF and RR scheduling policies. Moreover, we study the frame structure optimization problem. For the sake of simplicity, we denote with Ψ the set of network parameters $\{N_{RN}, \bar{d}, \mathcal{B}, P_{RN}\}$, and we focus in this section on a given Ψ.

A. Stations and Sector Throughput

We define here the *average sector throughput*, which is our objective function for comparing different network configurations. We start with intermediate definitions.

Definition 1 (Average sum physical data rate)**.** *For a set of network parameters Ψ and a station $k \in \mathcal{S}$, we define the average sum physical data rate as the expectation over frames of the sum of all data rates delivered to its served users:*

$$H_k \triangleq \mathbb{E}_n[\sum_{i\in\mathcal{U}_k(n)} R_{i,k}(n)]. \quad (11)$$

In this definition, $\mathbb{E}_n[f(n)] = \lim_{N_F\to\infty} 1/N_F \sum_{n=1}^{N_F} f(n)$ indicates the average over time frames of a function f. Over time, randomness is due to the number of served UEs, UE locations, shadowing and fast fading. In particular, note that $\mathcal{U}_k(n)$ is the random set that collect all UEs served by k in frame n.

Definition 2 (Average station throughput)**.** *For a set Ψ, a station $k \in \mathcal{S}$ and a given frame structure $\underline{\tau} = (\tau_1, ..., \tau_{N_{RN}})$, we define the average station throughput as the expectation over frames of the sum of throughputs delivered to its served users:*

$$\bar{T}_k(\underline{\tau}) = \begin{cases} \min\left\{t_a\mathbb{E}_n\left[\sum_{i\in\mathcal{U}_k(n)} R_{i,k}(n)\right]; \tau_k\mathbb{E}_n\left[R_{BL,k}(n)\right]\right\} \\ \qquad \textit{for } k\in\mathcal{S}_{RN}, \\ t_a\mathbb{E}_n\left[\sum_{i\in\mathcal{U}_k(n)} R_{i,k}(n)\right] \\ \qquad \textit{for } k=0. \end{cases} \quad (12)$$

Contrary to the definition of the average sum physical throughput, the average station throughput takes into account the bottleneck represented by the BL for relay stations. This definition is still valid for out-of-band relays provided that we adopt the convention that in this case $\tau_k\mathbb{E}_n[R_{BL,k}(n)] = \infty$. Note that we have: $\bar{T}_k(\underline{\tau}) = \min\{t_aH_k; \tau_k\mathbb{E}_n[R_{BL,k}(n)]\}$ for $k \in \mathcal{S}_{RN}$ and $\bar{T}_0(\underline{\tau}) = t_aH_0$. In case of out-of-band relays, we have $t_a = 1$ and $\bar{T}_k(\underline{\tau}) = H_k$ for all k.

Definition 3 (Average sector throughput)**.** *For a set Ψ, a sector consisting of one eNB sector and N_{RN} relays, and a frame structure $\underline{\tau}$, we define the average sector throughput as the sum of sector stations throughputs:*

$$C(\underline{\tau}) = \sum_{k\in\mathcal{S}} \bar{T}_k(\underline{\tau}) = t_aH_0 + \sum_{k\in\mathcal{S}_{RN}} \min\{t_aH_k; \tau_k\mathbb{E}_n[R_{BL,k}(n)]\}. \quad (13)$$

Again, we adopt the convention that $\tau_k\mathbb{E}_n[R_{BL,k}(n)] = \infty$ for all k when out-of-band relays are considered. Recall that $R_{BL,k}(n)$ is given by (10).

Fast fading is a phenomenon that considerably increases the simulation time. This is due to the fact that it has varies on a much faster time-scale (few ms) than shadowing or UE locations. In the following sections, we thus propose a statistical method for taking into account fast fading without explicitly simulating it. In particular, we analyze H_k under PF and RR scheduling assumptions.

B. Station Throughput Under RR Scheduling

With RR scheduling, every station provides in every frame all its served UEs with an equal share of resource blocks, uniformly distributed in the frame for each UE, and selected regardlessly of the fast fading realization. Under these assumptions, the PDF $\Phi_{\theta^2}(x)$ of θ^2 experienced by the UE scheduled on a given resource block is given by $\Phi_{\theta^2}(x) = e^{-x}$. We have the following result:

Proposition 1 (Average sum physical data rate under RR scheduling)**.** *Under the assumption that all stations in $\mathcal{S}$ adopt the RR scheduling, the average sum physical data rate of station $k \in \mathcal{S}$ can be written as:*

$$H_k = \sum_{v=0}^{N_U} \binom{N_U}{v} p_k^v (1-p_k)^{N_U-v} v\mathbb{E}_\Omega\left[\frac{1}{A_k}\int_{\mathcal{A}_k} \frac{\mathcal{L}_\rho(\frac{1}{\beta\Gamma_k(s)})}{\beta\Gamma_k(s)} ds\right], \quad (14)$$

with

$$\mathcal{L}_\rho(s) = \frac{\alpha e^s}{s\ln(2)}\left[-\ln(\bar{t}+1)e^{-s(\bar{t}+1)} + E_1(s) - E_1(s(\bar{t}+1))\right] + \frac{\rho_{min}e^{-s\bar{t}}}{s}, \quad (15)$$

where $\bar{t} = 2^{\frac{\rho_{min}}{\alpha}} - 1$, $E_1(x) = \int_x^\infty \frac{e^{-u}}{u}du$, $\Gamma_k(s)$ is the SINR of a UE located in s and served by k, p_k is the probability for a UE to be served by k, and expectation is taken over shadowing variations (with respect to random variable Ω).

Proof. see Appendix A. □

We use (14) in our simulations with several realizations of the shadowing. Parameter p_k is obtained as a ratio of the serving surface to the network surface (assuming uniform UE distribution) and the integral is numerically obtained over the surface of station k (which is constant for a realization of shadowing random variables). We see from this approach that fast fading is not explicitly simulated although its effect is taken into account.

C. Station Throughput Under PF Scheduling

If stations have perfect Channel State Information (CSI) regarding their UEs, a PF scheduler can be used to assign resources blocks to all UEs served by a given station during a frame. Adopting the PF scheduler definition of [43], the PF scheduler assigns each slot to the UE enjoying the best fast fading conditions. We have thus:

$$\begin{aligned}\Phi_{\theta^2}(x) &= ve^{-x}\left(1-e^{-x}\right)^{v-1}, \\ &= ve^{-x}\sum_{r=0}^{v-1}\binom{v-1}{r}(-1)^r e^{-rx}, \qquad (16)\end{aligned}$$

where v is the number of UEs served by k.

Proposition 2 (Average sum physical data rate under PF scheduling)**.** *Under the assumption that all stations in $\mathcal{S}$ adopt the PF scheduling, the average sum physical data rate of station $k \in \mathcal{S}$ can be written as (using the notations of Proposition 1):*

$$\begin{aligned}H_k &= \sum_{v=0}^{N_U}\sum_{r=0}^{v-1} p_k^v\left(1-p_k\right)^{N_U-v} v^2\binom{v-1}{r} \times \\ &\quad (-1)^r \mathbb{E}_\Omega\left[\frac{1}{A_k}\int_{\mathcal{A}_k}\frac{\mathcal{L}_\rho\left(\frac{r+1}{\beta\Gamma_k(s)}\right)}{\beta\Gamma_k(s)}ds\right]. \qquad (17)\end{aligned}$$

Proof. see Appendix B. □

Again, we obtain an expression for H_k based on average SINR, avoiding fast fading explicit simulation.

D. Frame Structure Optimization

We now want to find the frame structure $\underline{\tau}^*$ that maximizes the sector throughput $C(\underline{\tau})$ for a network configuration Ψ.

Lemma 1 (Upper bound for τ_k^*)**.** *The optimal frame structure $\underline{\tau}^*$ is such that $\tau_k^* \in [0;\tau_{k,max}]$ where:*

$$\tau_{k,\max} = \frac{t_a H_k}{\mathbb{E}_n\left[R_{BL,k}(n)\right]}. \qquad (18)$$

Proof. Consider RN k. As we see from (12), BL k data rate linearly increases with τ_k, while RL k data rate linearly decreases with τ_k. As a consequence, the maximum data rate is obtained for $\tau_k = \tau_{k,\max}$, where $\tau_{k,\max}$ is the value of τ_k for which BL k and RL k data rates are equal. We have that, if $\tau_k > \tau_{k,\max}$, then the BL can deliver to the RN more data than those that the RN can deliver to its UE. Thus, a part of BL-dedicated resource blocks do not carry data and they are wasted. Hence, $\tau_{k,\max}$ represents an upper bound for τ_k^*. □

In the following, we assume that $\tau_k \leq \tau_{k,\max}$, $\forall k \in \mathcal{S}_{RN}$. Under this constraint, (12) can be rewritten as:

$$\bar{T}_k(\underline{\tau}) = \begin{cases}\tau_k \mathbb{E}_n\left[R_{BL,k}(n)\right\}, & \text{for } k \in \mathcal{S}_{RN}, \\ t_a H_k, & \text{for } k = 0.\end{cases} \qquad (19)$$

Corollary 1 (Optimal frame structure)**.** *For a given network configuration Ψ, define $\Delta_k(\Psi) = \mathbb{E}_n\left[R_{BL,k}(\Psi,n)\right] - H_0(\Psi)$, $k \in \mathcal{S}_{RN}$. If $\Delta_k(\Psi) > 0$ for all $k \in \mathcal{S}_{RN}$, then the optimal frame structure is $\underline{\tau}^* = (\tau_{1,max},\ldots,\tau_{N_{RN},max})$ and the optimal sector throughput is given by:*

$$C_{\max}(\Psi) = H_0(\Psi) + \sum_{k\in\mathcal{S}_{RN}}\tau_{k,\max}(\Psi)\Delta_k(\Psi). \qquad (20)$$

Proof. In the following we explicitly recall that the considered performance parameters depend on the network configuration Ψ. Considering (19), (13) can be expressed as:

$$\begin{aligned}C(\underline{\tau},\Psi) &= t_a H_0(\Psi) + \sum_{k\in\mathcal{S}_{RN}}\mathbb{E}_n\left[R_{BL,k}(\Psi,n)\right]\tau_k (21)\\ &= H_0(\Psi) + \sum_{k\in\mathcal{S}_{RN}}\tau_k\Delta_k(\Psi),\end{aligned}$$

where $\tau_k \in [0,\tau_{k,\max}(\Psi)]$. Parameters $H_0(\Psi)$ and $\Delta_k(\Psi)$ are completely determined by network setup Ψ, while τ_k, $k \in \mathcal{S}_{RN}$ can be tuned in order to maximize $C(\underline{\tau},\Psi)$. Now sector throughput $C(\underline{\tau},\Psi)$ is a multilinear function of the τ_k, which is non decreasing in every τ_k since we have assumed that $\Delta_k(\Psi) > 0$. As a consequence, it achieves its maximum for $\tau_k = \tau_{k,\max}(\Psi)$. □

Note that the condition $\Delta_k(\Psi) > 0$ for all k is not very restrictive. Indeed, assume that for some k_0, $\Delta_{k_0}(\Psi) \leq 0$. Then, $C(\underline{\tau},\Psi)$ is optimized by setting $\tau_{k_0} = 0$ because it is a non increasing function of τ_{k_0}. This means that we do not dedicate any resource on the BL to k_0, when Δ_{k_0} is negative, leaving k_0 inactive. This case does not make sense in a practical context, where RNs are deployed in order to be used and to obtain a benefit in terms of, e.g., throughput, coverage, etc. Hence, we do not consider such configurations in our work, which focuses on configurations Ψ for which condition $\Delta_k(\Psi) > 0$, $\forall k \in \mathcal{S}_{RN}$ is fulfilled.

Note also that $\underline{\tau}^*$ optimizes the frame structure in terms of *average* sector throughput. This can be justified by the fact that the frame structure is set for a long term and cannot be changed dynamically. As we assume that all sectors are statistically identical, the optimized frame is valid for all sectors. This results in a synchronized frame structure across sectors and cells.

E. Desirability of Relaying

We now propose a simple condition to be checked to know whether a network configuration Ψ is desirable, i.e., whether it is worth deploying relays with Ψ rather than not deploying relays.

Proposition 3. *A network configuration Ψ is desirable w.r.t. the case where no relays are deployed iff:*

$$\left(H_0(\Psi) + \sum_{k\in\mathcal{S}_{RN}}H_k(\Psi)\right)\left(1 - \sum_{k\in\mathcal{S}_{RN}}\tau_{k,\max}(\Psi)\right) > \tilde{H}_0, \qquad (22)$$

where $\tilde{H}_0$ is the average sum physical data rate of the eNB sector when no relays are deployed.

Proof. Starting from (20), we can state that relaying is desirable in terms of sector throughput if and only if

$$\begin{aligned}\tilde{H}_0 &< H_0(\Psi) + \sum_{k\in\mathcal{S}_{RN}}\tau_{k,\max}(\Psi)\Delta_k(\Psi), \\ &< H_0(\Psi) + (1 - \sum_{k\in\mathcal{S}_{RN}}\tau_{k,\max}(\Psi)) \times \\ &\quad \sum_{k\in\mathcal{S}_{RN}}\frac{H_k(\Psi)}{\mathbb{E}_n\left[R_{BL,k}(\Psi,n)\right]}\left(\mathbb{E}_n\left[R_{BL,k}(\Psi,n)\right] - H_0(\Psi)\right), \\ &< (H_0(\Psi) + \sum_{k\in\mathcal{S}_{RN}}H_k(\Psi))(1 - \sum_{k\in\mathcal{S}_{RN}}\tau_{k,\max}(\Psi)).\end{aligned}$$ □

We see that the condition (22) highlights the contribution of the proportion of resources dedicated to the backhaul (the

TABLE I
ANALYZED RANGE OF VALUES FOR N_{RN}, P_{RN}, $\mathcal{B}$ AND $\bar{d}$.

Parameter	Explored Interval	Step
N_{RN}	[1 , 7]	1
P_{RN}	[21 , 46] dBm	5 dBm
$\mathcal{B}$	[0 , 15] dB	3 dB
$\bar{d}$	[0.01 ISD , 0.25 ISD]	0.01 ISD

factor: $1 - \sum_{k \in \mathcal{S}_{RN}} \tau_{k,\max}(\Psi)$) and of the increase of the number of network stations (with the sum: $\sum_{k \in \mathcal{S}_{RN}} H_k(\Psi)$) to the desirability of RNs deployment. From (18), $\tau_{k,max}$ increases with the station k's delivered data rate and decreases with the backhaul quality. For out-of-band relays, the factor $1 - \sum_{k \in \mathcal{S}_{RN}} \tau_{k,\max}(\Psi)$ reduces to 1 and there is no influence of the BL. The sum $\sum_{k \in \mathcal{S}_{RN}} H_k(\Psi)$ is the result of network densification, which is known to increase system capacity [44].

V. NUMERICAL RESULTS AND DISCUSSION

A. Simulation Procedure

We describe here how the evaluation of $C_{\max}(\Psi)$ is carried out, for any considered set of network parameters $\Psi : \{N_{RN}, \bar{d}, \mathcal{B}, P_{RN}\}$. Monte Carlo simulations are used to obtain numerical results. At each iteration n the following operations are performed:

1) The simulator drops N_U UEs in the network with uniform spatial distribution. Shadowing realizations are drawn between any station-UE pair and between eNB sectors and associated RNs.
2) A serving station is associated to each UE, considering the bias factor $\mathcal{B}$.
3) The SINR $\Gamma_{i,k}(n)$ between every UE and its serving station is computed with (5) and recorded. In the same way, the SINR $\Gamma_{k,h}(n)$ in (9) between the eNB sector and every RN is computed and used to compute $R_{BL,k}(n)$ from (10).

After 1000 iterations, $\mathbb{E}_n[R_{BL,k}]$ is obtained by averaging all recorded $R_{BL,k}(n)$. Then, H_k is computed according to the chosen scheduling policy with (14) or (17). In these equations, p_k is obtained with the proportion of UEs served by k along the iterations and the integral is obtained by averaging the integrand over UEs served by k. At last, the optimal frame structure is derived from (18). Any Ψ not fulfilling conditions of Corollary 1 or of Proposition 3 is discarded (the configuration is said *not valid*).

Simulations are repeated for several Ψ, in order to find the set yielding the best performance in terms of sector throughput $C_{max}(\Psi)$. In particular, the analyzed range of values for each parameter are indicated in Table I. In this table, ISD stands for Inter-Site Distance, i.e., the distance between two neighboring eNBs. We considered values of P_{RN} up to 46 dBm, as high power relay nodes are considered as a viable solution in particular contexts, e.g., in rural areas [45].

B. Simulations Settings

Simulations performed in this paper are compliant with simulation parameters given in [4, case 1], if not otherwise specified (see Table II). The network cluster used to simulate a real network is formed by two cell rings around a central cell. Moreover, the wraparound technique has been employed (six cell clusters are 'wrapped' around the central cluster). All the measurements are carried out on UEs dropped uniformly in every cell of the central cluster, which are assumed to be always in Non Line Of Sight (NLOS) with respect to network stations. We denote as *load* the number of UEs dropped in each cell at each simulation snapshot.

TABLE II
SIMULATIONS SETTINGS

Parameter	Value
Cell rings	2
P_{eNB}	46 dBm
eNB antenna gain	14 dBi
RN antenna gain	5 dBi
UE antenna gain	0 dBi
$\rho_{\max}$	4.4 bit/s/Hz
β	1
α	0.6
σ_{RL}	10 dB
σ_{BL}	0 dB (LOS), 6 dB (NLOS)
σ_{DL}	8 dB
UE noise figure	9 dB
RN noise figure	5 dB
η_{RL}	3.75
η_{BL}	2.35 (LOS), 3.63 (NLOS)
η_{DL}	4.28
Antenna Pattern (horizontal)	$-\min[12(\phi/\phi_{3dB})^2, A_m]$, $A_m = 25dB, \ \phi_{3dB} = 70°$

We consider the case of in-band and out-of-band relaying. For in-band relaying, we consider two models for the Backhaul Link (BL): 1) 'LOS BL': RNs are always in Line Of Sight (LOS) with respect to their serving eNB, and always in NLOS with respect to interfering eNBs, as in, e.g., [8]. The 'LOS BL' can be considered as a 'good' backhaul link. 2) '3GPP BL': RNs can be in LOS or NLOS with respect to their serving eNB with a certain probability, depending on the distance. The same holds for interfering eNBs (see [4, case 1]). '3GPP BL' can be seen as a 'bad' backhaul link.

C. Out-of-Band Relaying

In this section, we analyze the out-of-band relaying case. Figure 4 shows sector throughput $C_{\max}$ vs N_{RN} for variable cell load, considering an ISD of 1 km, and for the best network configuration Ψ. $C_{\max}$ steadily increases with N_{RN}, because radio resources available for UEs transmission in the cell increase with N_{RN}, i.e., the network becomes more *dense*. Moreover, we do not need to use part of radio resources for the BL, as in the case of in-band relaying. The impact of network densification on $C_{\max}$ overcomes that of an increased amount of transmitting RNs, which negatively affects the SINR experienced by UEs. This phenomenon is less accentuated for low cell load. Indeed, in this case adding more RNs has less positive effect on cell throughput, because there is a non-negligible probability that a RN do not control any UE.

Note that scheduling gain grows with N_{RN}, when cell load is high (75 UEs per cell). Indeed, due to the increase of relays, interference increases and the average experienced SINR is slightly degraded. Authors of [43] have shown that when the spectral efficiency is upper bounded (as it is the case here with parameter ρ_{max}), a lower average SINR leads to a higher scheduling gain, which explains the observed

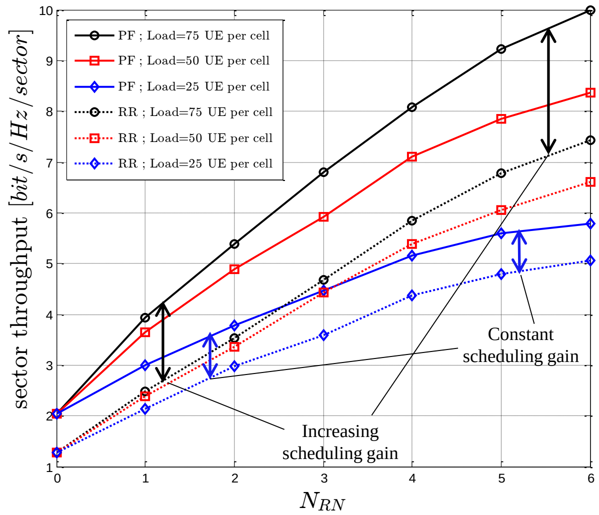

Fig. 4. $C_{\max}$ vs N_{RN} (out-of-band relaying, Inter-Site Distance (ISD) is 1 km).

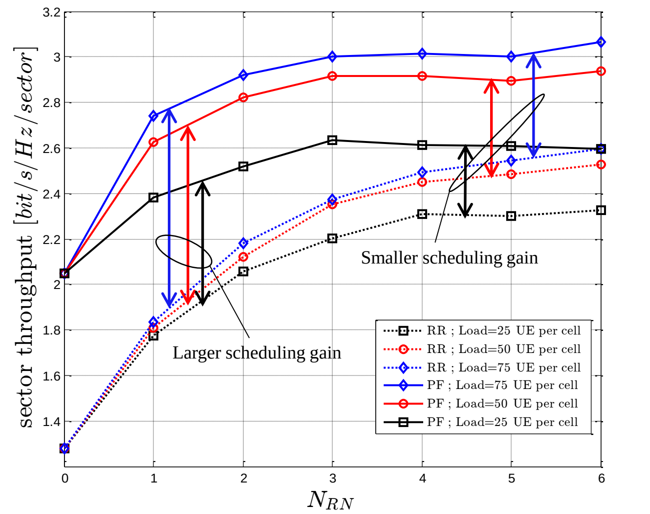

Fig. 6. $C_{\max}$ vs N_{RN} for variable load (in-band relaying, Inter-Site Distance (ISD) is 1 km, Line Of Sight Backhaul Link model 'LOS BL').

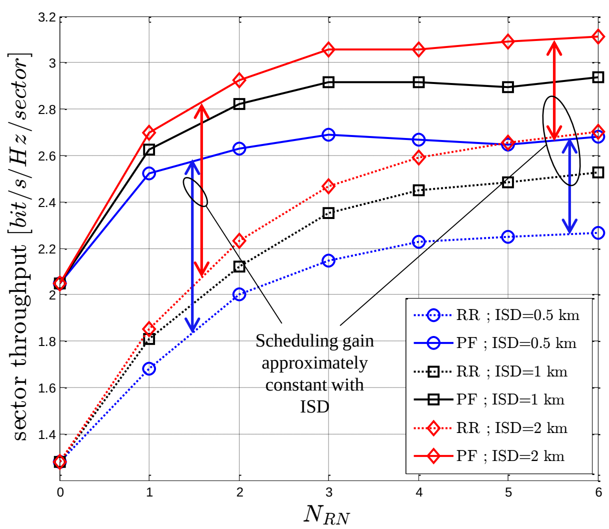

Fig. 5. $C_{\max}$ vs N_{RN} (in-band relaying, 50 UEs per cell, Line Of Sight Backhaul Link model 'LOS BL').

tendency[4]. Instead, when cell load is lower (e.g., 25 UEs per cell), scheduling gain remains approximately constant with N_{RN}, because RNs control few UEs (or no UEs at all), and hence we have little UEs diversity gain.

The optimized value of P_{RN}, found through simulations, is 46 dBm (the highest value in the tested range), for all N_{RN} and scheduling policies, when out-of-band relaying is adopted. This is due to the fact that backhaul does not limit performance in the out-of-band case. Thus, RNs can support a high number of UEs without any penalty in terms of capacity. Power $P_{RN} = 46$ dBm tends to equally balance the number of UEs served by eNB sectors and RNs.

[4]Imagine on the contrary that SINRs are so high for all UEs that their data rate is always ρ_{max}, then there is no scheduling gain of PF over RR.

D. In-Band Relaying

Figure 5 plots the value of $C_{\max}$ vs N_{RN} for different ISDs (for a load of 50 UEs per cell), showing the effect of a change in cell dimension on scheduling gain. As we can see, $C_{\max}$ grows with ISD (see also e.g. [46]), because interference has a lower impact on performance compared to thermal noise. Moreover, backhaul capacity decreases less rapidly with ISD, compared to RL capacity, as η_{BL} is lower on the useful signal in LOS (2.35) than on the interference (3.63 in NLOS). However, RNs control more UEs (in average) when ISD increases. This is because $\eta_{RL} < \eta_{DL}$. Thus, scheduling gain for UEs served by RNs grows, while the behavior of scheduling gain for UEs served by the eNB sector tends to decrease, resulting in no meaningful variations of the overall scheduling gain with respect to ISD.

Figure 6 shows the value of $C_{\max}$ and of the scheduling gain vs N_{RN} for different cell loads, when in-band relaying is adopted and a LOS backhaul model is used. The quantity of resources dedicated to backhaul link has a decisive effect on performance. Sector throughput $C_{\max}$ constantly increases with N_{RN}, when RR scheduling is adopted, while, for PF scheduling, $C_{\max}$ stops increasing for $N_{RN} \approx 3$. This is explained by the fact that PF scheduling applied to RNs implies a higher quantity of data to be transmitted to UEs, because of the increased scheduling performance. Hence, we have a higher data demand on the backhaul link, which negatively affects performance. The higher τ overcompensates the benefit of network densification in equation (22).

It can be observed that the scheduling gain decreases with N_{RN}. This is again due to the higher backhaul link data rate required by PF scheduler-equipped RNs. Thus, PF scheduling largely outperforms RR when few RNs are deployed, while RR scheduling performance approaches that of PF when N_{RN} grows.

The optimal value of P_{RN} for in-band relaying is 46 dBm for small N_{RN}, while optimal P_{RN} decreases for high N_{RN}.

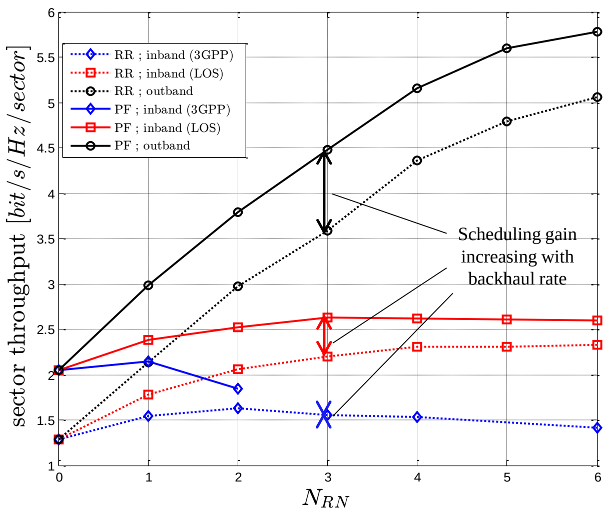

Fig. 7. $C_{\max}(\Psi)$ vs N_{RN} for different backhaul models (3GPP Backhaul Link '3GPP BL', Line Of Sight Backhaul Link 'LOS BL' and outband backhaul), Inter-Site Distance (ISD) is 1 km.

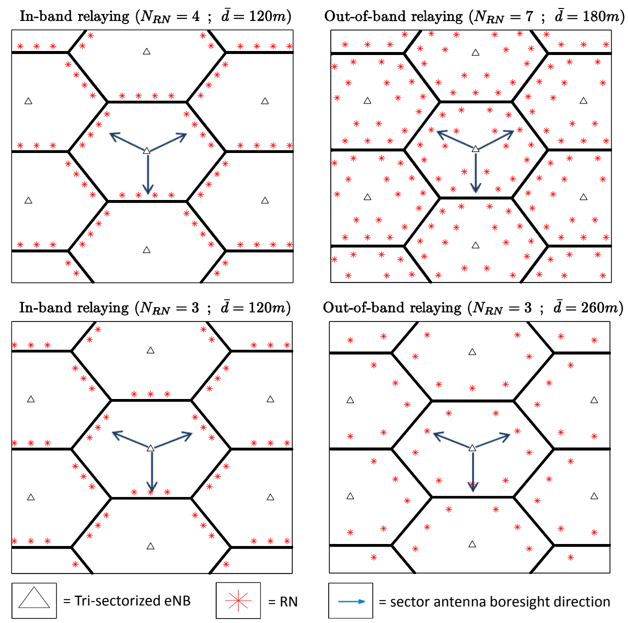

Fig. 8. Examples of optimized RNs placement (ISD=1km, 'LOS BL' model for in-band relays, 25 UEs per cell).

We can explain this result with the fact that, if N_{RN} and P_{RN} are both high, the quantity of UEs controlled by RNs is such that backhaul link consumption, in terms of radio resources, makes this solution not desirable. Hence, P_{RN} must be decreased, in order to balance the number of UEs controlled by RNs.

E. Influence of Backhaul Quality

Figure 7 plots $C_{\max}$ vs N_{RN} for the different Backhaul Link (BL) models defined in Section V-B (for an ISD of 1 km and a load of 25 UEs per cell), and shows how the scheduling gain increases with BL quality, and the decisive influence of BL on performance. When the worst performing BL type is adopted ('3GPP BL'), PF scheduling does not gain much, or even performs worse than RR scheduling. This can be explained by the fact that PF scheduling adopted by RNs implies a higher rate demanded by RNs on the BL. The increase in τ may overcompensate for the increase in UEs instantaneous rates, and network capacity decreases. If '3GPP BL' is adopted, optimization procedure cannot find any scenario complying with condition of Proposition 3, for some values of N_{RN}. This is the reason for the points missing in one curve of Figure 7.

F. RNs placement

Figure 8 shows examples of optimized RNs placement, for $N_{RN} = 3, 4, 7$ and for both in-band and out-of-band cases and optimized Ψ. Reference distance $\bar{d}$ tends to be smaller for in-band relaying, while it grows for out-of-band relaying as we can see for $N_{RN} = 3$. This is due to the fact that eNB antenna gain decreases with the distance from eNB sector antenna boresight direction. Hence, in-band RNs tend to group close to the boresight direction, in order to have a high backhaul rate. This effect is dominant with respect to the need for RNs to be more uniformly distributed in the cell, in order to increase UEs average experienced SINR. This latter exigence solely determines the RNs placement optimization when out-of-band relaying is adopted, i.e., there is no concern about backhaul rate.

For the in-band case, although relays are grouped together around antenna boresight direction, it is still desirable to deploy RNs with respect to the no relay case. There is indeed a diversity effect with respect to shadowing: UEs located close to the clustered RNs have a high probability to enjoy a good shadowing on the link towards one of the clustered RNs. This benefits them in terms of serving station received power.

In our experiments, we noticed how optimized RNs placement weakly depends on the adopted scheduling policy. This may be due to the fact that a change in RNs placement mainly affects RNs backhaul rate (for in-band relaying) and the cell regions covered by each RN. Both of these parameters do not depend on scheduling.

G. Coverage

Figure 9 plots the 5th %-ile of UE rate vs N_{RN} for in-band and out-of-band relaying, corresponding to the optimized RNs placement scenarios. We note that in the out-of-band relaying there is a consistent improvement of cell-edge rate given by RNs deployment, while in the in-band relaying case the coverage remains roughly constant. This is again due to the backhaul-related capacity penalty which is related to in-band relaying: the effect of densification and of the improvement of cell-edge UEs SINR is compensated by τ. Backhaul also affects the scheduling gain in terms of coverage, which is lower for the in-band relaying case.

H. Comparison with Simulated Annealing

In this section, we numerically compare the results obtained by the proposed heuristic and SA in one of our scenarios. In Figure 10, we compare the optimal sector throughput as computed by the proposed heuristic and SA for the same

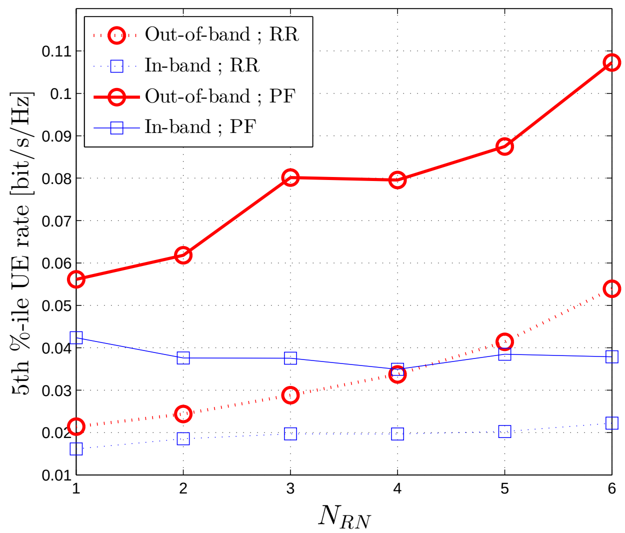

Fig. 9. Coverage related to optimized RNs placement (ISD=1km, 'LOS BL' model for in-band relays, 25 UEs per cell).

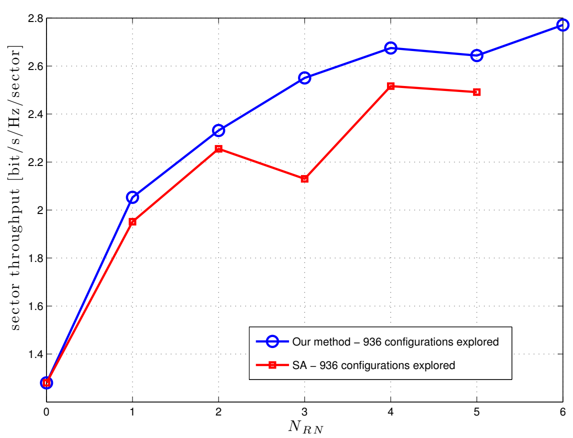

Fig. 10. Comparison between the proposed heuristic and Simulated Annealing in terms of sector throughput (RR scheduling, 75 UEs per cell, in-band relaying with '3GPP BL' backhaul link model).

number of iterations. The temperature decrease is proportional to $\log(k+1)$ after k iterations. With our simulation settings, we have $P = 6$, $B = 6$ and $\bar{d}$ varies in $[0.01ISD, 0.25ISD]$ with steps of $0.01ISD$, i.e., $D = 26$. This results in $P \times B \times D = 936$ iterations for our heuristic. We observe that our approach and SA provide similar results when the number of relays is small. However, when this number increases, SA fails to find good solutions because the search space is much larger. In our simulation, SA was not even able to find a valid configuration for 6 relays. Of course, the number of iterations should be increased in this case, but for a fixed number of iterations, our algorithm is more efficient.

VI. Conclusions

We have analyzed the impact of different scheduling policies on performance of relay-enhanced LTE-A cellular networks. A network model has been proposed, and expressions for stations throughput and sector throughput have been derived, for PF and RR scheduling. We have derived the optimal frame structure for throughput maximization and proposed a sub-optimal relay placement heuristic, which accelerates the optimization process. Results show that PF does not bring a consistent performance improvement with respect to RR, in several scenarios, e.g., when 1) many RNs are deployed and in-band relaying is adopted, or 2) backhaul rate is low, or 3) the network load is low and out-of-band relaying is adopted. Relays placement optimization is strongly influenced by the backhaul: in-band relays tend to group around sector antenna boresight direction, while for out-of-band relays tend to be more uniformly distributed in the sector.

Appendix A
Proof of Proposition 1

Let start from the definition of H_k in (11) and of $R_{i,k}(n)$ in (7), assuming that fast fading follows the PDF $\Phi_{\theta^2}(x) = e^{-x}$:

$$\begin{aligned} H_k &= \mathbb{E}_n \sum_{i\in\mathcal{U}_k(n)} \int_0^\infty \min\{\alpha \log_2(1+\beta\Gamma_{i,k}(n)x), \rho_{min}\} e^{-x} dx \\ &= \mathbb{E}_n \sum_{i\in\mathcal{U}_k(n)} \int_0^\infty \min\{\alpha \log_2(1+t), \rho_{min}\} e^{-\frac{t}{\beta\Gamma_{i,k}(n)}} \frac{dt}{\beta\Gamma_{i,k}(n)} \\ &= \mathbb{E}_n \sum_{i\in\mathcal{U}_k(n)} \frac{\mathcal{L}(\min\{\alpha\log_2(1+t),\rho_{min}\})\left(\frac{1}{\beta\Gamma_{i,k}(n)}\right)}{\beta\Gamma_{i,k}(n)}, \end{aligned} \tag{23}$$

where $\mathcal{L}(f(t))(s) = \int_0^\infty e^{-st} f(t) dt$ is the Laplace transform (a similar approach is used in [32]). Let denote $\mathcal{L}_\rho(s) \triangleq \mathcal{L}(\min\{\alpha\log_2(1+t), \rho_{min}\})(s)$ and let $\bar{t}$ be the value for which we have $\alpha\log_2(1+t) = \rho_{min}$, i.e., $\bar{t} = 2^{\frac{\rho_{min}}{\alpha}} - 1$. We have:

$$\begin{aligned} \mathcal{L}_\rho(s) &= \int_0^{\bar{t}} e^{-st}\alpha\log_2(1+t)dt + \rho_{min}\int_{\bar{t}}^\infty e^{-st}dt \\ &= \frac{\alpha e^s}{\ln(2)}\int_1^{\bar{t}+1} e^{-sh}\ln(h)dh + \frac{\rho_{min}e^{-s\bar{t}}}{s} \\ &= \frac{\alpha e^s}{s\ln(2)}\left[-\ln(\bar{t}+1)e^{-s(\bar{t}+1)} + E_1(s) - E_1(s(\bar{t}+1))\right] \\ &\quad + \frac{\rho_{min}e^{-s\bar{t}}}{s}, \end{aligned} \tag{24}$$

where we used the identity $\int e^{ax}\ln(x)dx = \frac{e^{ax}\ln(x)}{a} - \frac{1}{a}\int \frac{e^{ax}}{x}dx$ and where $E_1(x) = \int_x^\infty \frac{e^{-u}}{u}du$. Now, when there are N_U users in the network, and denoting p_k the probability for a UE to be served by k, we have from (23):

$$\begin{aligned} H_k &= \sum_{v=0}^{N_U}\binom{N_U}{v} p_k^v (1-p_k)^{N_U-v} \times \\ &\quad \mathbb{E}_n\left[\sum_{i\in\mathcal{U}_k}\frac{\mathcal{L}_\rho(\frac{1}{\beta\Gamma_{i,k}(n)})}{\beta\Gamma_{i,k}(n)}\,\middle|\, |\mathcal{U}_k| = v\right] \\ &= \sum_{v=0}^{N_U}\binom{N_U}{v} p_k^v (1-p_k)^{N_U-v}\, v \times \\ &\quad \mathbb{E}_\Omega\left[\frac{1}{A_k}\int_{\mathcal{A}_k}\frac{\mathcal{L}_\rho(\frac{1}{\beta\Gamma_k(s)})}{\beta\Gamma_k(s)}ds\right], \end{aligned} \tag{25}$$

where $\Gamma_k(s)$ is the SINR of a UE located in s and served by k. We used here the fact that UE spatial distribution is uniform and so the expectation over n knowing v is v times the average value for a UE uniformly distributed over the serving area. The only remaining source of randomness is shadowing. □

APPENDIX B
PROOF OF PROPOSITION 2

We start again from the the definition of H_k in (11) and of $R_{i,k}(n)$ in (7), assuming that fast fading follows the PDF $\Phi_{\theta^2}(x) = ve^{-x}(1-e^{-x})^{v-1}$ (a similar approach is followed in [13], [32], [33]) when k serves v users:

$$\begin{aligned}
H_k &= \sum_{v=0}^{N_U} \binom{N_U}{v} p_k^v (1-p_k)^{N_U-v} \times \\
&\quad \mathbb{E}_n \left[\sum_{i\in\mathcal{U}_k} \int_0^\infty \min\{\alpha \log_2(1+\beta\Gamma_{i,k}(n)x), \rho_{min}\} \times \right. \\
&\quad \left. ve^{-x} \sum_{r=0}^{v-1} \binom{v-1}{r} (-1)^r e^{-rx} dx \,\middle|\, |\mathcal{U}_k| = v \right] \\
&= \sum_{v=0}^{N_U} \binom{N_U}{v} p_k^v (1-p_k)^{N_U-v} \times \\
&\quad \mathbb{E}_n \left[\sum_{i\in\mathcal{U}_k} \sum_{r=0}^{v-1} v \binom{v-1}{r} (-1)^r \frac{\mathcal{L}_\rho(\frac{r+1}{\beta\Gamma_{i,k}(n)})}{\beta\Gamma_{i,k}(n)} \,\middle|\, |\mathcal{U}_k| = v \right] \\
&= \sum_{v=0}^{N_U} \sum_{r=0}^{v-1} p_k^v (1-p_k)^{N_U-v} v^2 \binom{v-1}{r} \times \\
&\quad (-1)^r \mathbb{E}_\Omega \left[\frac{1}{A_k} \int_{\mathcal{A}_k} \frac{\mathcal{L}_\rho(\frac{r+1}{\beta\Gamma_k(s)})}{\beta\Gamma_k(s)} ds \right].
\end{aligned} \quad (26)$$

□

REFERENCES

[1] Z. Hasan, H. Boostanimehr, and V.K. Bhargava. Green cellular networks: A survey, some research issues and challenges. *Communications Surveys Tutorials, IEEE*, 13(4):524–540, Nov. 2011.

[2] P.-C. Lin, R.-G. Cheng, and Y.-J. Chang. A dynamic flow control algorithm for LTE-Advanced relay networks. *Vehicular Technology, IEEE Transactions on*, 63(1):334–343, Jan. 2014.

[3] ITU-R IMT. Requirements, evaluation criteria and submission templates for the development of IMT-Advanced, Dec. 2008.

[4] 3GPP. TR 25.816 v9.0.0 - Technical Specification Group Radio Access Network; Evolved Universal Terrestrial Radio Access (E-UTRA); Further advancements for E-UTRA physical layer aspects (Release 9) - (2010-03), Dec. 2010.

[5] 3GPP TSG-RAN WG R1-094041 (CMCC). Relay performance evaluation, Oct. 2009.

[6] O. Bulakci and A. B. Saleh. Performance of relays in LTE-Advanced networks. *Technical presentation available on www.ikr.uni-stuttgart.de/Content/itg/fg524/Meetings/2010-02-18-Darmstadt/index.html*, Feb. 2010.

[7] A. Damnjanovic, J. Montojo, Yongbin Wei, Tingfang Ji, Tao Luo, M. Vajapeyam, Taesang Yoo, Osok Song, and D. Malladi. A survey on 3GPP heterogeneous networks. *Wireless Communications, IEEE Transactions on*, 18(3):10–21, Jun. 2011.

[8] W. Guo and T. O'Farrell. Relay deployment in cellular networks: Planning and optimization. *Selected Areas in Communications, IEEE Journal on*, 31(8):1597 – 1606, Aug. 2013.

[9] M. Salem A. Adinoyi M. Rahman H. Yanikomeroglu D. Falconer Y.-Doo Kim W. Shin E. Kim. Fairness-aware joint routing and scheduling in OFDMA-based cellular fixed relay networks. *IEEE International Conference on Communications (ICC)*, pages 1–6, Jun. 2009.

[10] R. Schoenen, R. Halfmann, and B.H. Walke. An FDD multihop cellular network for 3GPP-LTE. In *IEEE Vehicular Technology Conference (VTC)*, pages 1990 –1994, May 2008.

[11] M. Salem, A. Adinoyi, M. Rahman, H. Yanikomeroglu, D. Falconer, and Young-Doo Kim. Fairness-aware radio resource management in downlink OFDMA cellular relay networks. *Wireless Communications, IEEE Transactions on*, 9(5):1628 –1639, May 2010.

[12] J. Xu and L. Qiu. Area power consumption in a single cell assisted by relays. In *IEEE/ACM International Conference on Cyber, Physical and Social Computing (CPSCom)*, pages 460 –465, dec. 2010.

[13] R. Combes, Z. Altman, and E. Altman. Self-organizing relays: Dimensioning, self-optimization, and learning. *Network and Service Management, IEEE Transactions on*, 9(4):487–500, Dec. 2012.

[14] Kyungmi Park, C.G. Kang, Daeyoung Chang, Seungho Song, Jongguk Ahn, and Jongtae Ihm. Relay-enhanced cellular performance of OFDMA-TDD system for mobile wireless broadband services. In *IEEE International Conference on Computer Communications and Networks (ICCCN)*, pages 430–435, Aug. 2007.

[15] P. Rost, G. Fettweis, and J.N. Laneman. Energy- and cost-efficient mobile communication using multi-cell MIMO and relaying. *Wireless Communications, IEEE Transactions on*, 11(9):3377–3387, Sep. 2012.

[16] Wern-Ho Sheen, Shiang-Jiun Lin, and Chia-Chi Huang. Downlink optimization and performance of relay-assisted cellular networks in multicell environments. *Vehicular Technology, IEEE Transactions on*, 59(5):2529–2542, Jun. 2010.

[17] F. Kelly. Charging and rate control for elastic traffic. *European Transactions on Telecommunications*, 8(1):33–37, 1997.

[18] Woo-Geun Ahn and Hyung-Myung Kim. Proportional fair scheduling in relay enhanced cellular OFDMA systems. In *IEEE International Symposium on Personal, Indoor and Mobile Radio Communications (PIMRC)*, pages 1–4, Sep. 2008.

[19] Nan Yang, M. Elkashlan, and Jinhong Yuan. Impact of opportunistic scheduling on cooperative dual-hop relay networks. *Communications, IEEE Transactions on*, 59(3):689–694, Mar. 2011.

[20] Kasun T. Hemachandra and Norman C. Beaulieu. Opportunistic scheduling in dual-hop multiuser relay networks in the presence of co-channel interference. In *IEEE Global Communications Conference (GLOBECOM)*, pages 4635–4640, Dec. 2012.

[21] Xiaoyi Liu, Haochuan Zhang, Xin Zhang, and Dacheng Yang. Outage performance of opportunistic scheduling in multiuser relay network with selective decode-and-forward relaying. In *IEEE Vehicular Technology Conference (VTC Spring)*, pages 1–5, May 2011.

[22] M. Minelli, M. Ma, M. Coupechoux, J.-M. Kelif, M. Sigelle, and P. Godlewski. Optimal relay placement in cellular networks. *IEEE Trans. on Wireless Communications*, 13(2):998–1009, Feb. 2014.

[23] Abdallah Bou Saleh, Ömer Bulakci, Stefano Redana, and Jyri Hämäläinen. On cell range extension in LTE-Advanced type 1 inband relay networks. *Wireless Communications and Mobile Computing*, Jun. 2013.

[24] S. Brueck. Heterogeneous networks in LTE-Advanced. In *Wireless Communication Systems (ISWCS), 2011 8th International Symposium on*, pages 171–175, Nov. 2011.

[25] Anzil A Rasheed and Stefan Wager. Cell range extension in LTE in-band relays: Analysis of radio link, subframe allocation and protocol performance of FTP traffic model. In *European Wireless, 2012. EW. 18th European Wireless Conference*, pages 1–6, Apr. 2012.

[26] Akihito Morimoto, Nobuhiko Miki, Hiroyuki Ishii, and Daisuke Nishikawa. Investigation on transmission power control in heterogeneous network employing cell range expansion for LTE-Advanced uplink. In *European Wireless, 2012. EW. 18th European Wireless Conference*, pages 1–6, Apr. 2012.

[27] B.A. Yasir, Gang Su, and N. Bachache. Range expansion for pico cell in heterogeneous LTE. In *Computer Science and Network Technology (ICCSNT), 2012 2nd International Conference on*, pages 1235–1240, Dec. 2012.

[28] A.B. Saleh, Ö. Bulakci, J. Hämäläinen, S. Redana, and B. Raaf. Analysis of the impact of site planning on the performance of relay deployments. *Vehicular Technology, IEEE Transactions on*, 61(7):3139–3150, Sep. 2012.

[29] Wenchi Cheng, Hailin Zhang, Liqiang Zhao, and Yongzhao Li. Energy efficient spectrum allocation for green radio in two-tier cellular networks. In *IEEE Global Telecommunications Conference (GLOBECOM)*, pages 1 –5, Dec. 2010.

[30] M. Pikhletsky, F. Khafizov, Jietao Zhang, and HongCheng Zhuang. Dynamic radio resource management for OFDMA-based relay enhanced cellular network. In *IEEE Global Telecommunications Conference (GLOBECOM)*, pages 1 –5, dec. 2011.

[31] X.T. Vu, M. Di Renzo, and P. Duhamel. Ber analysis of joint network/channel decoding in block rayleigh fading channels. In *IEEE*

International Symposium on Personal Indoor and Mobile Radio Communications (PIMRC), pages 698–702, Sept 2013.

[32] B. Blaszczyszyn and M.K. Karray. Fading effect on the dynamic performance evaluation of OFDMA cellular networks. In *IEEE First International Conference on Communications and Networking (ComNet)*, pages 1 –8, nov. 2009.

[33] R. Combes, Z. Altman, and E. Altman. On the use of packet scheduling in self-optimization processes: Application to coverage-capacity optimization. In *IEEE Intl. Symposium on Modeling and Optimization in Mobile, Ad Hoc, and Wireless Networks (WiOpt)*, pages 11–20, Jun. 2010.

[34] D. Ben Cheikh, J.-M. Kelif, M. Coupechoux, and P. Godlewski. SIR distribution analysis in cellular networks considering the joint impact of path-loss, shadowing and fast fading. *EURASIP Journal on Wireless Communications and Networking*, 2011(137):1–10, Oct. 2011.

[35] P. Mogensen, Wei Na, I.Z. Kovacs, F. Frederiksen, A. Pokhariyal, K.I. Pedersen, T. Kolding, K. Hugl, and M. Kuusela. LTE capacity compared to the Shannon bound. In *IEEE Vehicular Technology Conference (VTC)*, pages 1234–1238, Apr. 2007.

[36] S. Boyd and L. Vandenbergh. *Convex Optimization*. Cambridge University Press, 2003.

[37] M. Chiang. Nonconvex optimization of communication systems. In D. Gao and H. Sherali, editors, *Advances in Mechanics and Mathematics, Special Volumn on Strang's 70th Birthday*. Springer, 2007.

[38] Z. Drezner and H. W. Hamacher. *Facility Location: Applications and Theory*. Springer-Verlag, 2004.

[39] K. Sambale and B. Walke. Decode-and-forward relay placement for maximum cell spectral efficiency. In *Proc. of IEEE European Wireless*, Apr. 2012.

[40] O. Catoni. Sharp large deviations estimates for simulated annealing algorithms. In *Annales de l'institut Henri Poincaré (B) Probabilités et Statistiques*, volume 27, pages 291–383. Gauthier-Villars, 1991.

[41] O. Catoni. Rough large deviation estimates for simulated annealing: Application to exponential schedules. *The Annals of Probability*, pages 1109–1146, 1992.

[42] O. Catoni. Applications of sharp large deviations estimates to optimal cooling schedules. In *Annales de l'institut Henri Poincaré (B) Probabilités et Statistiques*, volume 27, pages 463–518. Gauthier-Villars, 1991.

[43] R. Combes, S-E Elayoubi, and Z. Altman. Cross-layer analysis of scheduling gains: Application to LMMSE receivers in frequency-selective rayleigh-fading channels. In *IEEE International Symposium on Modeling and Optimization in Mobile, Ad Hoc and Wireless Networks (WiOpt)*, pages 133–139, May 2011.

[44] J.-M. Kelif and M. Coupechoux. Cell Breathing, Sectorization and Densification in Cellular Networks. In *Proc. of IEEE Int. Symp. on Modeling and Optimization in Mobile, Ad Hoc, and Wireless Networks (WiOPT)*, June. 2009.

[45] S. Sesia, I. Toufik, and M. Baker. LTE - The UMTS long term evolution: From theory to practice. *John Wiley & Sons*, page 675, Jan. 2009.

[46] L. Rong, S.E. Elayoubi, and O.B. Haddada. Impact of relays on LTE-Advanced performance. In *IEEE International Conference on Communications (ICC)*, pages 1–6, May 2010.

Mattia Minelli received his Master degree in telecommunications engineering from Politecnico di Milano in Italy, in 2009. He is currently participating in a Joint PhD Program between the School of Electrical and Electronic Engineering at Nanyang Technological University in Singapore and the Computer and Network Science Department of Telecom ParisTech in Paris. His research interests include wireless networks, propagation and radio resource management issues, and relaying in OFDMA networks.

Ma Maode received his PhD degree in computer science from Hong Kong University of Science and Technology in 1999. Now, Dr. Ma is an Associate Professor in the School of Electrical and Electronic Engineering at Nanyang Technological University in Singapore. He has extensive research interests including wireless networking and network security. Dr. Ma has more than 250 international academic publications including over 100 journal papers and more than 130 conference papers. He currently serves as the Editor-in-Chief of *International Journal of Electronic Transport*. He also serves as an Associate Editor for other five international academic journals. Dr. Ma is an IET Fellow and a senior member of *IEEE Communication Society* and *IEEE Education Society*. He is the vice Chair of the *IEEE Education Society*, Singapore Chapter. He is also an *IEEE Communication Society Distinguished Lecturer*.

Marceau Coupechoux has been working as an Associate Professor at Telecom ParisTech since 2005. He obtained his Masters' degree from Telecom ParisTech in 1999 and from University of Stuttgart, Germany, in 2000, and his Ph.D. from Institut Eurecom, Sophia-Antipolis, France, in 2004. From 2000 to 2005, he was with Alcatel-Lucent. He was a Visiting Scientist at the Indian Institute of Science, Bangalore, India, during 2011–2012. Currently, at the Computer and Network Science department of Telecom ParisTech, he is working on cellular networks, wireless networks, ad hoc networks, cognitive networks, focusing mainly on radio resource management and performance evaluation.

Philippe Godlewski received the Engineers degree from Telecom Paris (formerly ENST) in 1973 and the PhD in 1976 from University Paris 6. He is Professor at Telecom ParisTech in the Computer and Network Science department. His fields of interest include Cellular Networks, Air Interface Protocols, Multiple Access Techniques, Error Correcting Codes, Communication and Information Theory.